Supporting Information

Hybrid Remote Quantum Dot/Powder Phosphor Layers for Display Backlights

Sofie Abe[1,2,3]; Jonas J. Joos[2,3] ; Lisa I. D. J. Martin[2,3] ; Zeger Hens[1,3] ; Philippe F. Smet[2,3]

[1]Physics and Chemistry of Nanostructures, Ghent University, Gent, Belgium
[2]LumiLab, Ghent University, Gent, Belgium
[3]Center for Nano and Biophotonics, Ghent University, Gent, Belgium

S.1. Materials and Methods

CdSe wurtzite core QDs

CdSe wurtzite core QDs with a mean diameter of 2.77 nm were synthesized according to a hot injection procedure adapted from literature [1] by mixing 0.139 g of cadmium oxide (CdO, Sigma Aldrich, >99.99%), 0.648 g of octadecylphosphonic acid (PCI Synthesis) and 6.00 g of trioctylphosphine oxide (Merck Millipore, for synthesis) in a 25 ml three-neck flask and stirring under nitrogen flow during 1 hour at 120°C. Next, 1.8 ml of trioctylphosphine (TOP, Strem, min. 90%) was injected after heating to 345 °C under nitrogen atmosphere. After further heating to 345 °C, 1 mL of a 1.7 M solution of selenium (Se, Alfa Aesar, 200 mesh, 99.999%) dissolved in TOP was injected. The reaction was quenched by a temperature drop induced by removing the heating mantle after 25 sec and by putting the flask in a water bath at 70°C. During cooling down, 5 ml toluene and 8 ml methanol were injected. Centrifugation at 3900 rpm for 1 min and resuspension of the obtained nanocrystals in toluene was followed by two more purification steps involving the addition of methanol, centrifugation at 3000 rpm for 3 min, and redispersion in toluene.

CdSe/CdS core-shell structures

CdSe/CdS core-shell structures were synthesized according to a seeded growth procedure.[2] A reaction flask containing a mixture of CdO, oleic acid (1.5 g) and TOPO (3.0 g) is kept under vacuum at 60 °C for about 1 hour. The resulting solution is heated under nitrogen until it becomes colorless, then 1.8 ml of TOP is injected. Next, the temperature is allowed to reach 330 °C, at which point a mixture of trioctylphosphine sulfide (TOP-S; S dissolved in TOP) and CdSe seeds are injected. The reaction is quenched after 3 to 5 minutes by adding 5 ml of toluene and cooling in a water bath. The as-synthesized nanocrystals are purified 3 times by a purification step consisting of precipitation with methanol, centrifugation and resuspension in toluene after discarding the supernatant.

S.2. CdSe core QDs: absorption spectroscopy

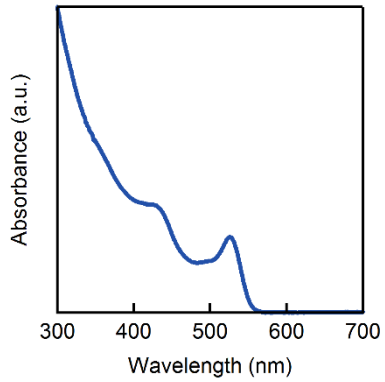

Figure S1. Normalized absorbance of a dilute dispersion of the CdSe core QDs.

S.3. CdSe/CdS core-shell QDs: Transmission Electron Micoscopy

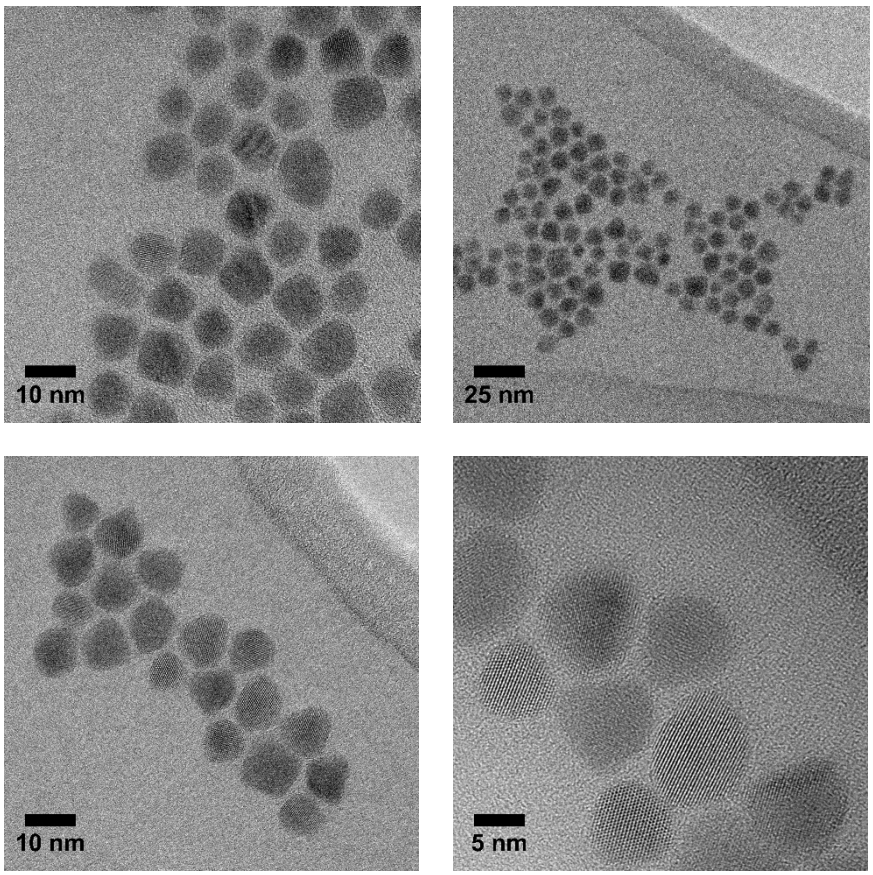

Figure S2. Transmission electron microscopy images of the obtained CdSe/CdS QDs – with thick CdS shell.

We used multiple images to measure the area of, in total, 70 particles, from which the equivalent diameter is calculated assuming sphere-shaped particles. For this particular suspension, we obtain d = 9.44 nm and σ_d = 1.29 nm (13.7%).

S.4. Roadmap to an efficient remote phosphor white LED for displays

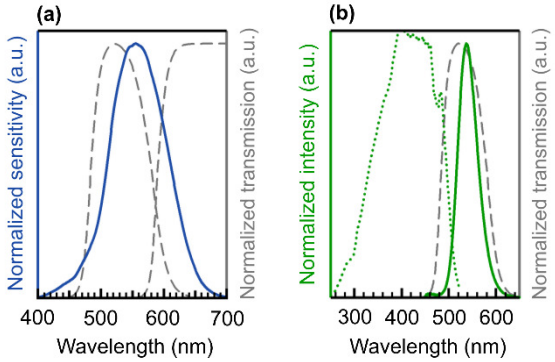

Figure S3. (a) Typical transmission spectrum of green and red color filter (gray dashed lines)[3, 4] and photopic eye sensitivity curve (blue full line). **(b)** Normalized excitation (green dotted line, measured at 534 nm) and emission (green full line, excited by 450 nm) spectra of STG powder. Typical transmission spectrum of green color filter (gray dashed line).

Saturated, green europium doped phosphor

Europium doped strontium thiogallate (STG) can be efficiently excited by blue light and shows a saturated green emission, which is ideal for displays as it can be used as primary with a minimum of additional color filtering (Figure S3b). Together with a short decay time, stability of emission color and conversion efficiency at elevated temperatures (up to 400 K), we can conclude that STG meets all important spectral requirements for conversion phosphors in display applications.[5-7]

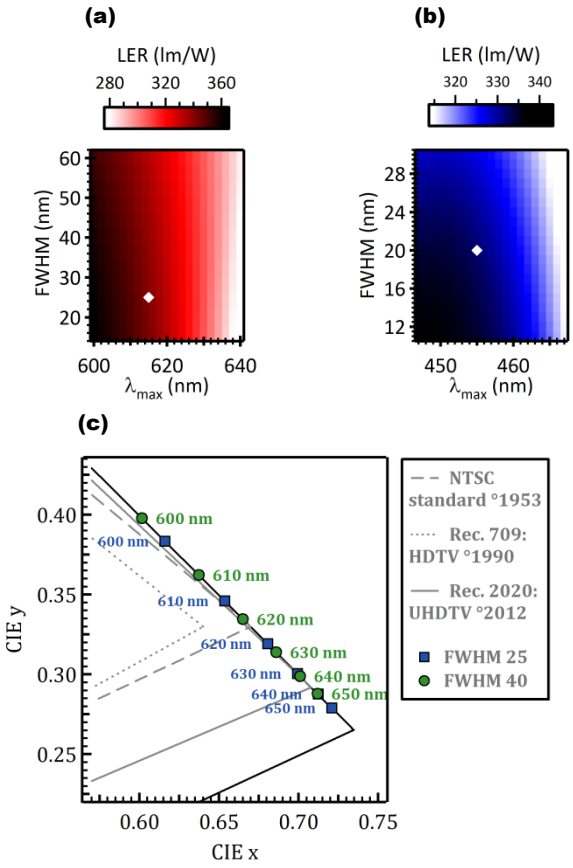

Figure S4. (a) Simulated influence of the spectral shape of the red QD emission on the LER of a three-band white LED with a CCT of 6500 K and $|D_{uv}| < 0.001$. The green component is the STG emission spectrum and the blue component a Gaussian curve with λ_{max} at 455 nm and a FWHM of 20 nm. The white diamond indicates the spectral shape of the red component used in the simulation of Figure 1b. **(b)** Simulated influence of the spectral shape of the blue component in a RGB LED on the LER for a CCT of 6500 K. The green component is the STG emission spectrum and the red component is a Gaussian curve with a λ_{max} at 615 nm and a FWHM of 25 nm. The white diamond indicates the spectral shape of the blue component used in the simulation of Figure 1b. **(c)** A zoom of the CIE 1931 chromaticity diagram shows in more detail the color points of QDs with a theoretical Gaussian emission profile with λ_{max} as denoted and a FWHM of 25 nm (blue squares) or 40 nm (green circles).

Red-emitting quantum dots

When aiming for the large color gamut determined by the UHDTV standard, the red emission should be as narrow as possible with a λ_{max} approaching 630 nm, as described in Rec. 2020. To avoid energy losses due to filtering, the red emission should not extend to wavelengths below 610 nm (Figure S3a). Quantum dots

are ideal candidates as red color convertor in displays since their FWHM is narrow (25 – 55 nm) and their emission maximum can be tuned precisely. As demonstrated for several simulated emission peaks with Gaussian shapes and a FWHM of either 25 or 40 nm in Figure S4c, the shift from the spectral locus is still relatively small for these emission widths. A wider emission band does however shift the color point away from the one aimed for in Rec. 2020, implying we need to increase λ_{max} above 640 nm. However, an emission reaching to longer wavelengths cannot be efficiently perceived by the human eye because the photopic eye sensitivity curve rapidly decreases around 610 nm (blue curve in Figure S3a). Therefore, an intermediate peak wavelength is required to balance a large color gamut and high efficiency. We performed a simulation of the influence of the spectral shape of a red emitting QD – simulated as a Gaussian emission profile with varying maximum and width – on the luminous efficacy of radiation (LER) of a pc wLED (Figure S4). For the green component we used the emission spectrum of STG and for the blue component a Gaussian curve with λ_{max} at 455 nm and a FWHM of 20 nm. The relative contribution of each RGB component was optimized for obtaining a maximal LER, while the CCT of the wLED was set at the Rec. 2020 target of 6500 K and the D_{uv} is kept between -0.001 and 0.001. The LER – indicated in lm/W_{opt} – obtained from the simulation is the theoretical maximal efficiency based solely on the shape of the wLED's emission spectrum. It is different from the luminous efficacy LE – expressed as lm/W_{el} – as it does not account for the radiant efficacy (W_{opt}/W_{el}) of the pumping LED and efficiency losses caused by color conversion with phosphors having an IQE below 100%. The results, which are graphically represented in Figure S4a, show that a λ_{max} between 620 and 630 nm in combination with a FWHM in the range 20 – 45 nm grants access to a LER of 308 – 332 lm/W and a proper color gamut, thereby giving a relevant target range of the QD's emission peak wavelength. Narrowing down the emission band has a positive effect on both the color gamut and LER.

Blue pumping LED

Typical characteristics of blue pumping LEDs used in literature are λ_{max} between 450 and 460 nm and FWHM of 20 – 28 nm.[8-12] Again, the choice for an optimal blue LED should be based on LER and color point.[8] A narrow emission profile with a maximum at short wavelengths ensures a large color gamut, but due to the shape of the spectral eye sensitivity, λ_{max} should not be below 445 nm. For the upper limit, a λ_{max} above 455 nm is not desirable as both the available color gamut and LER decrease exceedingly with increasing wavelength (Figure S4b). A similar conclusion was found for the blue component in wLEDs with low CCT.[13]

Summary

In conclusion, for a hybrid wLED using STG phosphor as saturated green color convertor we recommend the use of a blue pumping LED with 445 nm < λ_{max} < 455 nm and a FWHM as narrow as possible (preferably < 20 nm) and QDs with 620 nm < λ_{max} < 630 nm and a narrow FWHM (preferably < 35 nm).

S.5. SEM-CL and EDX of color convertor layers

Backscattered electron images of cross sections to determine layer thicknesses

Table S1. Results of SEM analysis of layers.

Type of layer	Average thickness (µm)	Standard deviation (µm)
Glass substrate	212	7
STG	286	16
QDs	294	34
STG+ QDs	317	42

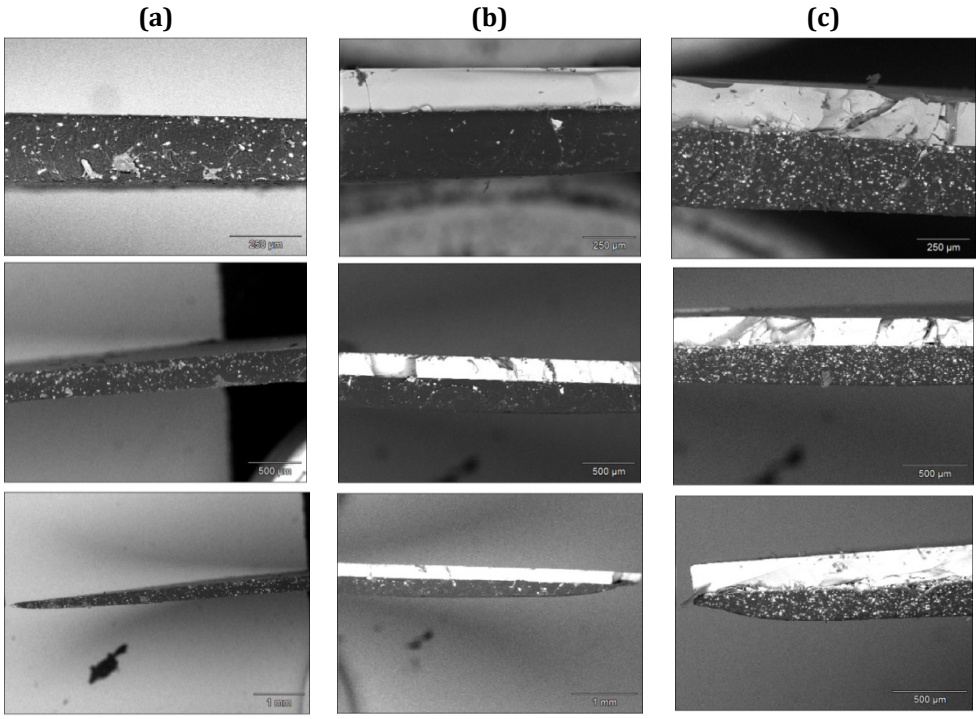

Figure S5. SEM images of a remote phosphor layer containing **(a)** only STG , **(b)** only CdSe/CdS QDs and **(c)** a mixture of both color convertors. The dark component is the polymer layer with phosphor powder and/or QDs, the light component is the glass substrate.

SEM-CL-EDX on single phosphor layers

It is interesting to get an idea about the spatial distribution of the color convertors in the polymer matrix and to link this to the luminescence properties of the entire layer by combining cathodoluminescence (CL) and energy dispersive X-ray spectroscopy (EDX) inside a scanning electron microscope (SEM).

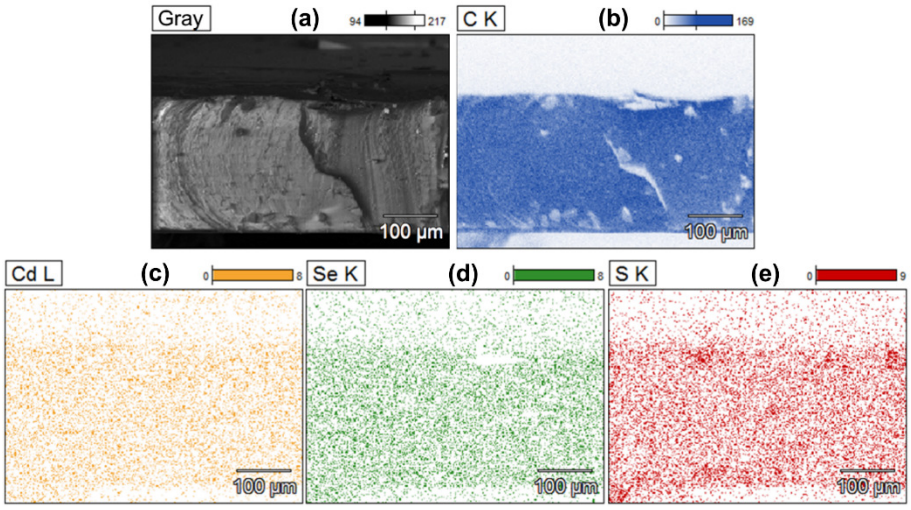

Figure S6 (a) Backscattered electron image of a phosphor layer containing 10 µl of CdSe/CdS QD stock solution, along with EDX maps for **(b)** carbon, **(c)** cadmium, **(d)** selenium and **(e)** sulfur. All data obtained at room temperature.

The CdSe/CdS QDs do not show efficient cathodoluminescence and their volume fraction in the polymer layer is too low to provide conclusive evidence on their exact distribution based on SEM-EDX (Figure S6). However, it is clear that the QDs did not aggregate on one side of the layer.

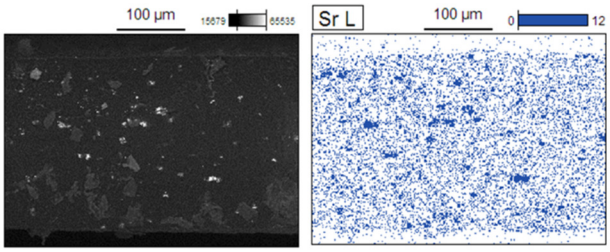

Figure S7. (left) Backscattered electron image of a phosphor layer containing 25 mg of STG powder, along with the EDX map of **(right)** strontium. All data are obtained at room temperature.

The backscattered electron image and corresponding EDX of a cross section of a layer containing 25 mg of STG powder, however, shows that the microcrystalline phosphor particles are distributed homogeneously over the layer, proving that they do not migrate to the bottom of the layer during the drying step (Figure S7).

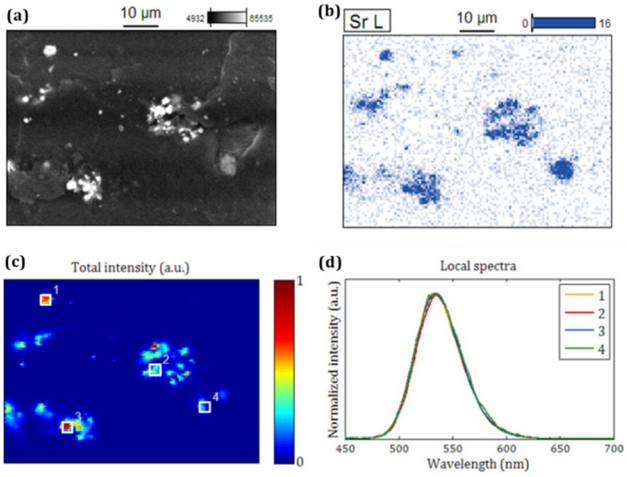

Figure S8. (a) Backscattered electron image of a phosphor layer containing 25 mg STG, along with EDX map for **(b)** strontium. **(c)** Maps for the emission intensity in the wavelength range (450–700 nm) relative to the total emission intensity. **(d)** Emission spectra for the four selected areas indicated in the CL map. All data are obtained at room temperature.

Figure S8a,b show the SEM and EDX results of a smaller area of the cross section. Some powder particles are located in clusters, while others are surrounded by polymer. The studied area was divided into 128 by 92 pixels and in each pixel a full CL emission spectrum was recorded (E = 15 keV) and is displayed in Figure S8d. In agreement with photoluminescence measurements, a λ_{max} of 535 nm and FWHM of 50 nm is obtained at the four indicated positions coinciding with STG particles (Figure S8c).

SEM-CL-EDX on mixed QD and STG phosphor layers

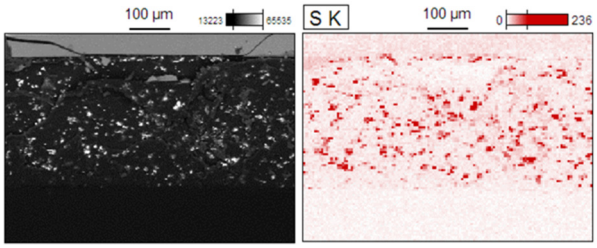

Figure S9 (left) Backscattered electron image of a phosphor layer containing 1 mg of STG powder and 10 µL CdSe/CdS QDs, along with EDX map of **(right)** sulfur. All data are obtained at room temperature.

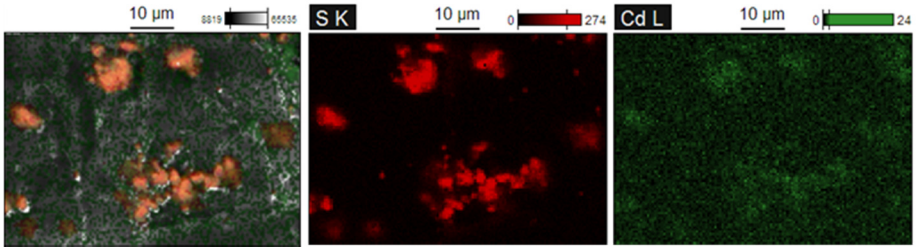

Figure S10 (left) EDX overlay map of a mixed hybrid layer containing 1 mg STG phosphor and 10 µL CdSe/CdS QDs, along with the EDX maps of its constituents **(middle)** sulfur and **(right)** cadmium. All data are obtained at room temperature.

S.6. Luminescence emission decay of color conversion layers

Table S2. Decay constants of red luminescence for phosphor layers and remote pc wLED configurations.

Name	τ_1 (ns)	f_1 (%)	τ_2 (ns)	f_2 (%)	τ_{av} (ns)
Diluted QD dispersion	108	75	833	25	286
$\|G_A\|$	486	100	-	-	486
$\|R_A\|$	117	80	716	20	235
$\|R_AG_A\|$	98	39	545	61	369
$\|R_A\|\|G_A\|$	120	80	678	20	230
$\|G_A\|\|R_A\|$	92	15	520	85	455
$\|R_A\|¦¦G_A\|$	113	79	683	21	233
$\|G_A\|¦¦R_A\|$	85	10	517	90	474

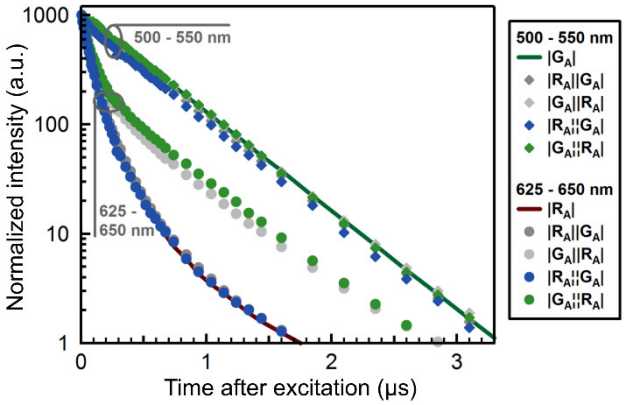

Figure S11. Decay of the green and red luminescence intensities. The full lines represent the decay of the color converting layers, the symbols the decay of the hybrid wLED configurations.

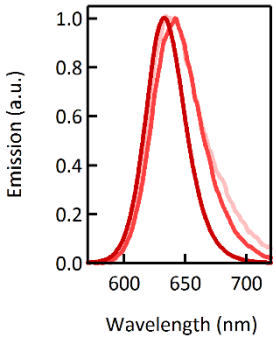

Figure S12. Emission spectra of a dilute QD dispersion (A = 10-20%) for different time intervals after excitation. Dark red = 0.00 – 0.05 µs, red = 0.5 – 0.7 µs, light red = 1.2 – 3.0 µs.

S.7. Scattering of STG layers

The scattering coefficient µ of the STG layers was calculated according to the formula [14]

$$\mu = -\frac{\log T}{d}$$

where T is the transmittance and d the thickness of the STG layer. The average transmittance was evaluated in the wavelength range from 600 to 625nm, where no absorption due to the STG occurs. T was obtained by measuring the transmitted light in the normal direction, with an opening angle of 3°. The thickness was derived from SEM measurement of cross-sections of the layers.

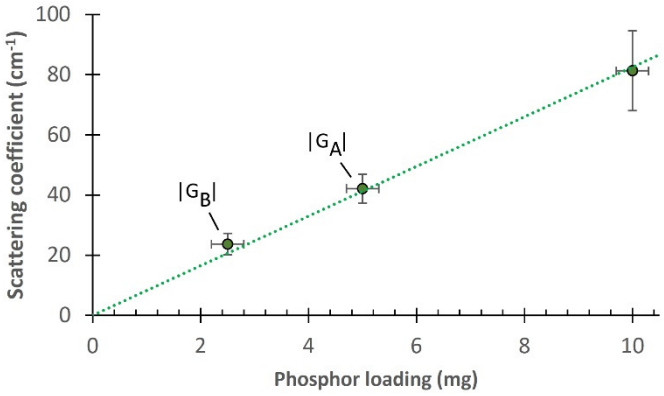

Figure S13. Scattering coefficient of the STG layers, as a function of phosphor loading.

S.8. Emission spectra of remote pc wLEDs with CCT ≈ 6500 – 7000 K

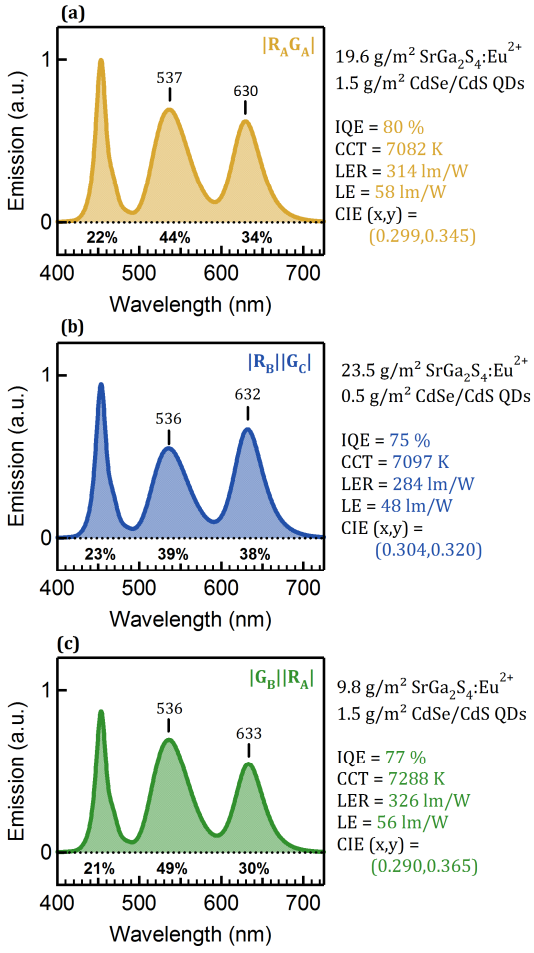

Figure S14. Emission spectrum, composition, efficiency, CCT, LER, LE and color point of a remote phosphor wLED composed of a blue pumping LED in a white mixing chamber containing **(a)** a hybrid phosphor layer |R_AG_A|, and layered configurations **(b)** |$R_B||G_C$|, and **(c)** |$G_B||R_A$|. The concentrations of color convertor material in each phosphor layer are indicated in Table 1 and 2.

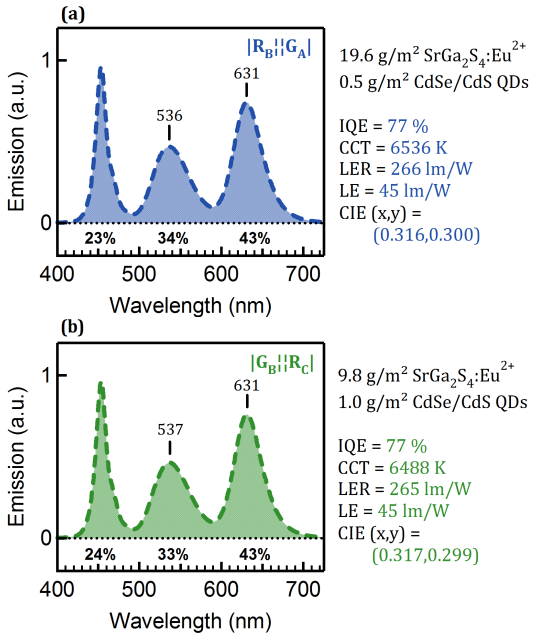

Figure S15. Emission spectrum, composition, efficiency, CCT, LER, LE and color point of a remote phosphor wLED composed of a blue pumping LED in a white mixing chamber containing layered configurations **(a)** $|R_B¦¦G_A|$ and **(b)** $|G_B¦¦R_A|$. The concentrations of color convertor material in each phosphor layer are indicated in Table 1 and 2.

S.9. References

1. Carbone L, Nobile C, De Giorgi M, Sala FD, Morello G, Pompa P, *et al.* Synthesis and Micrometer-Scale Assembly of Colloidal CdSe/CdS Nanorods Prepared by a Seeded Growth Approach. *Nano Lett* 2007; **7:** 2942-2950.

2. Cirillo M, Aubert T, Gomes R, Van Deun R, Emplit P, Biermann A, *et al.* Flash Synthesis of CdSe/CdS Core-Shell Quantum Dots. *Chem Mater* 2014; **26:** 1154-1160.

3. Xie RJ, Hirosaki N, Takeda T. Wide Color Gamut Backlight for Liquid Crystal Displays Using Three-Band Phosphor-Converted White Light-Emitting Diodes. *Appl Phys Exp* 2009; **2:** 022401.

4. Luo Z, Xu D, Wu ST, Emerging Quantum-Dots-Enhanced LCDs. *J Disp Technol* 2014; **10:** 526-539.

5. Joos JJ, Meert KW, Parmentier AB, Poelman D, Smet PF. Thermal Quenching and Luminescence Lifetime of Saturated Green $Sr_{1-x}Eu_xGa_2S_4$ Phosphors. *Opt Mater* 2012; **34:** 1902-1907.

6. Smet PF, Parmentier AB, Poelman D. Selecting Conversion Phosphors for White Light-Emitting Diodes. *J Electrochem Soc* 2011; **158:** R37-R54.

7. Chartier C, Barthou C, Benalloul P, Frigerio JM. Photoluminescence of Eu^{2+} in $SrGa_2S_4$. *J Lumin* 2005; **111:** 147-158.

8. Luo Z, Chen Y, Wu ST. Wide Color Gamut LCD with a Quantum Dot Backlight. *Opt Exp* 2013; **21:** 26269.

9. Jang E, Jun S, Jang H, Lim J, Kim B, Kim Y. White-Light-Emitting Diodes with Quantum Dot Color Converters for Display Backlights. *Adv Mater* 2010; **22:** 3076-3080.

10. Woo JY, Kim K, Jeong S, Han CS. Enhanced Photoluminance of Layered Quantum Dot–Phosphor Nanocomposites as Converting Materials for Light Emitting Diodes. *J Phys Chem C* 2011; **115:** 20945-20952.

11. Shin MH, Hong HG, Kim HJ, Kim YJ. Enhancement of Optical Extraction Efficiency in White LED Package with Quantum Dot Phosphors and Air-Gap Structure. *Appl Phys Exp* 2014; **7:** 052101.

12. Iffalovic PES, Adanova DOB, Ojtko ANV, Ergel MAJ, Odas MAH, Elletta MAP, *et al.* Evaluation of Low-cadmium ZnCdSeS Alloyed Quantum Dots for Remote Phosphor Solid-State Lighting Technology. *Appl Opt* 2015; **54:** 7094-7098.

13. Joos JJ, Botterman J, Smet PF. Evaluating the Use of Blue Phosphors in White LEDs: the Case of $Sr_{0.25}Ba_{0.75}Si_2O_2N_2:Eu^{2+}$. *J Sol Stat Lighting* 2014; **1:** 6.

14. Park HK, Oh JH, Do YR. Toward scatter-free phosphors in white phosphor-converted light-emitting diodes. *Opt Exp* 2012; **20:** 10218-10228.